Available online at www.sciencedirect.com

ScienceDirect

Energy Procedia 54 (2014) 549 – 556

Energy Procedia

4th International Conference on Advances in Energy Research 2013, ICAER 2013

Crystalline Zinc Indium Selenide Thin Film Electrosynthesis and its Photoelectrochemical Studies

Anuradha. B. Bhalerao [a]*, B.G.Wagh[b], N.M. Shinde [c], S. B. Jambure[c], C.D.Lokhande[c]

[a] *Applied Science Department, K.K. Wagh Institute of Engineering Education and Research, Nasik, M.S., India*
[b] *Department of Physics, K. K. Wagh College of Arts, Commerce and Science, Pimpalgaon, Nasik, M.S. India*
[c] *Thin Film Physics Lab, Department of Physics, Shivaji University, Kolhapur, M.S., India.*

Abstract

A room temperature electrochemical synthesis of Zinc Indium Selenide ($ZnIn_2Se_4$) thin films has been carried out. The films were polycrystalline and exhibited n-type conductivity. $ZnIn_2Se_4$ films were found to be photoactive in polysulphide solution. The photo electrochemical (PEC) studies of these films have been carried out using current-voltage (I-V) characteristics, power output characteristics, spectral response, Mott-Schottky plot and electrochemical impedance spectroscopy (EIS).

Selection and peer-review under responsibility of Organizing Committee of ICAER 2013

Keywords: Zinc indium selenide, Electrochemical synthesis, X-ray diffraction, Scanning electron microscopy, Photoelectrochemical cell.

1. Introduction

The fabrication of p–n junction solar cells has already been achieved with high degree of sophistication, but in 1970's, an alternative way of solid–liquid junction was suggested. Semiconductor liquid junction solar cells have been attracting a great deal of attention during last few years due to growing interest in solar energy conversion [1]. As compared to solid–solid junction of conventional solar cells, a semiconductor electrode dipped in a suitable liquid electrolyte provides the necessary charge transfer. A redox ionic species are being used to obtain

* Corresponding author. Tel: +91-0253- 2314030, Fax: +91-0253-2511962
E-mail address: anuradhapawar@gmail.com, acpawar@kkwagh.edu.in

Selection and peer-review under responsibility of Organizing Committee of ICAER 2013
doi:10.1016/j.egypro.2014.07.296

photovoltage/photocurrent. After a little modification, solid-liquid junction has in-built storage capability. Semiconductor electrolyte interface may be used for photo electrolysis, photo catalysis, and photoelectrochemical (PEC) power conversion [2]. The semiconducting thin film electrode like zinc indium selenide ($ZnIn_2Se_4$) has been studied due to its wide applications in solar cells and optoelectronic devices [3-4]. The $ZnIn_2Se_4$ is n-type semiconducting ternary chalcogenide of the type $A^{II}B^{III}{}_2\,C^{VI}{}_4$, where A = Zn, Cd or Hg, B = In or Ga, and C = S, Se, Te [5].

Soliman and Nahass have studied optical properties of $ZnIn_2Se_4$ films grown by thermal evaporation technique on quartz substrate [6]. Later Hendia and Soliman studied effect of deposition rate on structural and optical properties of the $ZnIn_2Se_4$ grown on glass substrate [7]. E. Nowak et al. reported electrical properties of $ZnIn_2Se_4$ thin films [8]. Xianzhong Sun et al. have grown $ZnIn_2Se_4$ buffer layer by thermal diffusion on $CuInSe_2$ thin film deposited by electrodeposition [9]. $ZnIn_2Se_4$ material has also been prepared by co-evaporation [10-12], chemical vapor deposition [13], spray pyrolysis [14, 15], and vertical Bridgman technique [16]. However, no attempt has been made for deposition of $ZnIn_2Se_4$ thin films by electrodeposition method. Literature survey reveals that n- type $ZnIn_2Se_4$ film electrode has not been reported as photoelectrode.

In this paper, we report the synthesis of n-$ZnIn_2Se_4$ film electrode on stainless steel substrates at ambient temperature. We studied PEC properties in polysulphide electrolyte, which may enable capability of ambient temperature fabrication of p–n junction diode or solar cell.

2. Experimental

All AR grade (Aldrich and Merck) chemicals were used for synthesis of $ZnIn_2Se_4$ film electrode. $ZnIn_2Se_4$ thin films were electrodeposited onto a stainless steel substrate (1x1 cm^2). The substrates were initially polished with zero grade polish paper and cleaned with labolene, and finally by an ultrasonic cleaner. The economical and inert polished graphite plate (5x 1x 0.2 cm^3) was used as a counter electrode. The molarities of precursor solutions of zinc sulphate ($ZnSO_4$), indium trichloride ($InCl_3$) and selenium dioxide (SeO_2) solutions were kept 0.2 M, 0.02 M, and 0.002 M respectively. The depositions were carried out from an unstirred solution (35 cc with precursor ratio 1:2:4) at room temperature under potentiostatic conditions with a saturated calomel electrode (SCE) as a reference electrode. As per pourbaix diagram, the pH of the bath was kept constant as 2.2 by adding few drops of 0.1M HCl [17]. The polarization curves were recorded for 0.2 M $ZnSO_4$, 0.02 M $InCl_3$ and 0.002 M SeO_2 separately and then from the bath having compositions of $ZnSO_4$, $InCl_3$ and SeO_2 in the volumetric proportions as 1:2:4.

The films deposited using optimized conditions were used for further characterization by X-ray diffraction (XRD), Scanning electron microscopy (SEM), UV-Visible spectroscopy, and PEC techniques. Photoelectrochemical characterization of $ZnIn_2Se_4$ thin films was carried out using a PEC cell configuration as $ZnIn_2Se_4$|0.1.M Polysulphide|C. The distance between working electrode and counter electrode was 0.5 cm. Photocurrent–voltage curves were measured under 50 mW/cm^2 light illumination intensity. The spectral response of the PEC cell was recorded with monochromator in the wavelength range of 350–800 nm. The speed of response of the cell was recorded as a rise and decay of photocurrent with time. Transient photoresponse of the cell was used to study decay constant. The capacitance–voltage (C–V) characteristics of the cell in terms of Mott–Schottky plot was used to determine the flat band potential (V_{fb}) of $ZnIn_2Se_4$ electrode.

3. Results and Discussion

3.1. Polarization Curve

A preliminary requirement for codeposition of two or more metals from the electrolyte is that at least one of them must be individually capable of being deposited from the bath. The most important practical consideration involved in the codeposition of three metals is that their deposition potentials must be fairly close together. In general, the potentials of the metals even in the solutions of various ions can be brought closer together by changing the concentrations of either the metals or pH of the bath [18]. The electrolyte bath consisting of aqueous solutions of 0.2 M $ZnSO_4$, 0.02 M $InCl_3$ and 0.002M SeO_2 in various proportions was used to deposit Zn-In-Se films at ambient

temperature. Fig. 1 shows the plots of polarization curves for reduction of zinc, indium, selenium and $ZnIn_2Se_4$ thin film which indicates cathodic deposition potential of 600mV Vs SCE for codeposition of zinc, indium and selenium.

The deposition conditions such as precursor solution proportion, deposition time and bath pH are optimized to achieve the uniform thickness adherent film. Further rise in these parameters resulted in decrease and non uniformity of film thickness. This may be attributed to the fact that after attaining the highest thickness (0.789µm) the films may have tensile stress, which causes delamination or peeling off the layer [19]. Another possible reason may be that the excess charge is used for side reactions only.

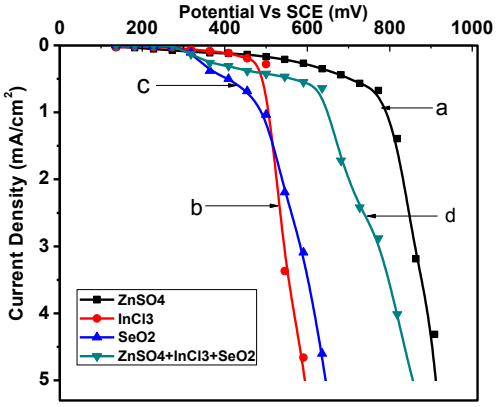

Fig. 1 Polarization curves for reduction of (a) zinc, (b) indium, (c) selenium and (d) for the bath containing precursor solutions in the ratio 1:2:4.

3.2. Crystal Structure and Surface Morphology

The X-ray diffraction pattern of the as deposited film electrode on stainless steel substrate is shown in Fig. 2. The XRD pattern shows remarkable texture growth structure along (2 2 0) and (1 1 2) planes, as evidenced by JCPDS data file card [39–1156] in addition to few other minor peaks viz. (3 0 1), (1 1 6) and (4 0 0).

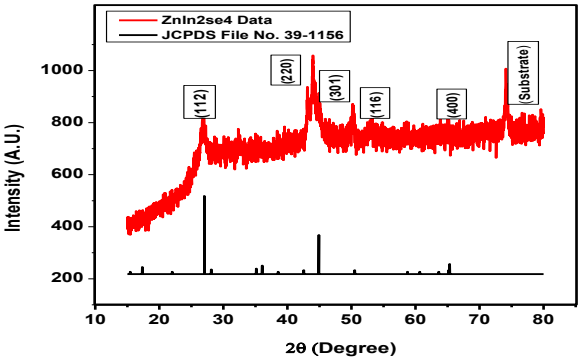

Fig. 2 The X-ray diffraction pattern of as-deposited $ZnIn_2Se_4$ thin film.

There was good matching between observed and standard interplanar spacing (d) values with tetragonal crystal structure and lattice parameters as (a=b= 5.7095Å, c= 11.449Å) suggesting the formation of $ZnIn_2Se_4$.

Fig. 3(a-b) shows the scanning electron micrograph (SEM) image of $ZnIn_2Se_4$ film electrode at magnifications 10,000x and 30,000x. Lower magnification image shows overgrown grains in some regions of the film. It shows a close packed structure with the average grain width and breadth falling in the nanometer range (about 500nm) and

length about 2000nm. An observation at higher magnification reveals well resolved uniform grain growth with good film coverage. The grains are compact with tetragonal (rod like) shape. These rods are aggregated to form homogeneous local edge-sharing network structure on substrate surface without void spaces.

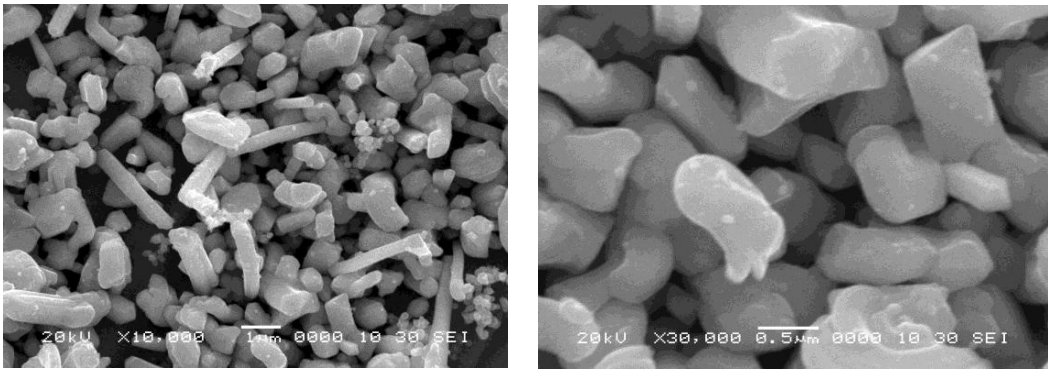

3(a) 3(b)

Fig.3 The scanning electron micrographs of $ZnIn_2Se_4$ film electrode at magnifications (a) 10,000 x and (b) 30,000x.

3.3. Optical Absorbance Study

The optical absorption spectrum of $ZnIn_2Se_4$ film deposited onto stainless steel substrate was studied at the room temperature in the wavelength of 300–800 nm. Fig.4 (inset) shows the variation of optical absorbance (αt) with wavelength. The absorption hump was found near 400 to 500nm region. $ZnIn_2Se_4$ shows absorbance in the visible region, which is the characteristic of $ZnIn_2Se_4$ to use it as absorber layer.

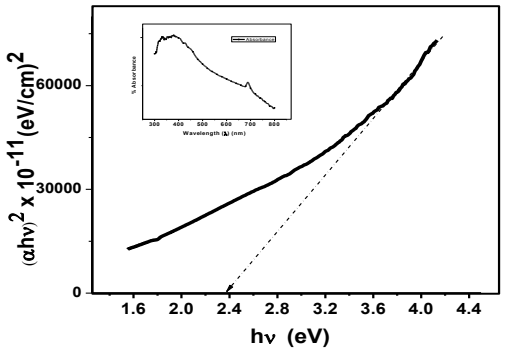

Fig.4 The plot of $(\alpha h\nu)^2$ versus (hν) of $ZnIn_2Se_4$ thin film.
(Inset shows the variation of absorption (αt) with wavelength (λ) of Zn In_2Se_4 thin film.)

The Energy band gap (E_g) was calculated using the Eq. (1)

$$\alpha = \frac{A(h\nu - Eg)^n}{h\nu} \qquad (1)$$

Where hν is the photon energy, A and n are constants. For allowed direct transition, n = 1/2 and for allowed indirect transition n = 2. Fig.4 shows the variation of $(\alpha h\nu)^2$ with (hν) for $ZnIn_2Se_4$ film. The linear nature of the plot indicates the existence of the direct transition. The band gap E_g was determined by extrapolating the straight portion to energy axis at α = 0. The band gap was found to be 2.4 eV for $ZnIn_2Se_4$ thin film, which is in good agreement

with the values reported earlier for the $ZnIn_2Se_4$ thin films [21]. This value is suitable for using $ZnIn_2Se_4$ thin film as an absorber layer of solar cell by selecting proper p- type partner and a buffer layer [20].

The observed value is greater than the reported band gap value (2.3 eV) of $ZnIn_2Se_4$ material [21] and film shows a blue shift of 0.1 eV in optical spectrum. This is attributed due to the size-quantization in nanocrystalline semiconductor [22]. This size quantization occurs due to localization of electrons and holes in a confined volume of the semiconductor nanocrystals. This results in a change in energy band structure, with separation of individual energy levels and an increase in effective optical 'band gap' of the semiconductor as compared with bulk value.

The optical absorption spectrum of $ZnIn_2Se_4$ film deposited onto stainless steel substrate was studied at the room temperature in the wavelength of 300–800 nm. Fig.4 (inset) shows the variation of optical absorbance (αt) with wavelength. The absorption hump was found near 400 to 500nm region. $ZnIn_2Se_4$ shows absorbance in the visible region, which is the characteristic of $ZnIn_2Se_4$ to use it as absorber layer.

3.4. Photoelectrochemical Cell Output Parameter

The PEC cell with the configuration, $ZnIn_2Se_4$|0.1 M polysulphide ($NaOH+Na_2S+S$) |C is formed. It is seen that PEC cell gives some dark voltage (V_d) and dark current (I_d) with $ZnIn_2Se_4$ electrode as the negative and graphite electrode as the positive polarity ends. The origin of this dark voltage is attributed to the difference between two half cell potentials in the PEC cells which can be written as in Eq. (2)

$$E = E_{graphite} - E_{ZnIn2Se4} \qquad (2)$$

Where $E_{graphite}$ and $E_{ZnIn2Se4}$ are the half cell potentials when dipped in the polysulphide electrolyte. After illumination of the junction, the magnitude of voltage increases with negative polarity towards the $ZnIn_2Se_4$ thin film and anodic behavior of semiconductor is observed which indicates that the conductivity of $ZnIn_2Se_4$ thin film is of n-type as shown in Fig.(5a)

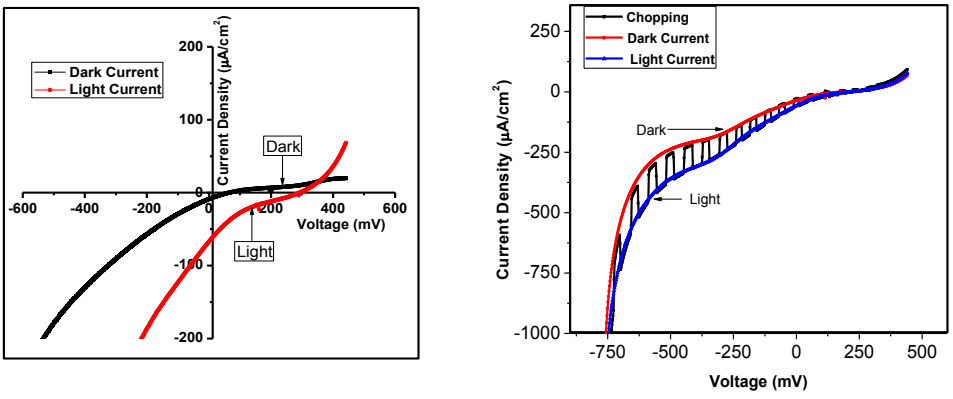

(a) (b)

Fig. 5 The Current–voltage (I–V) characteristic in dark and under light illumination (a) photovoltaic power output characteristics and (b) light chopping.

Photoelectrochemical cell (PEC) is based on the junction between semiconductor and an electrolyte. An electrolyte plays an important role in PEC cell which acts as a medium for charge transfer between the photoelectrode and counter electrode [23]. The PEC response under chopped light (50 mW/cm^2) conditions was carried out in order to study the photosensitivity of the $ZnIn_2Se_4$ thin film. The photoresponse of film was carried out by forming a typical configuration cell n- $ZnIn_2Se_4$ (stainless steel substrate) | 0.1 M polysulphide |graphite. Fig.5(b) shows well defined anodic (n-type) photoactivity under illumination. The photosensitivity confirmed that $ZnIn_2Se_4$ can be used as n-type absorber layer in a solar cell.

The low photocurrents have been attributed to high band gap, while the photosensitivity of the material is the result of rod like morphology. Such morphology provides easier electron transport path than percolation through the random spherical nanoparticles. This increases electron diffusion length with enhanced photochemistry as reported by Law et al. [24].

3.5. Electrode surface wettability study

The wettability test is carried out, in order to study the interaction between electrode and electrolyte. The wetting behavior is characterized by the value of the contact angle, a microscopic parameter. If the wettability is high, contact angle (θ), will be small and the surface is hydrophilic. On the contrary, if the wettability is low, θ will be large and the surface is hydrophobic. The contact angle is an important parameter in surface science and its measurement provides a simple and reliable technique for the interpretation of surface energies. The method involves the measurement of contact angle between water and the thin film electrode. The contact angle is expected to depend upon local inhomogeneity, chemical composition and the surface morphology of the semiconducting electrodes. Fig. 3c shows the water contact images of $ZnIn_2Se_4$ film. The contact angle for $ZnIn_2Se_4$ thin film is found to be 85.4°.This indicates that $ZnIn_2Se_4$ electrode material is hydrophilic in nature, which will be responsible for formation of better interfacial region in PEC cell.

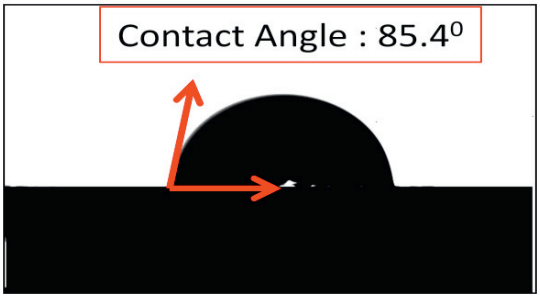

Fig. 6 Contact angle measurement for studying $ZnIn_2Se_4$ electrode-electrolyte interfacial region

3.6. Speed of Response and Transient Photoresponse Characteristics

Speed response of PEC cell was measured as a plot of photocurrent as a time (Fig. 7a). It is noteworthy that rapid rise and fall of current makes feasible to use this material as a light sensor. The slope observed in phase change region is attributed to film thickness which increases intercalation and deintercalation period. Speed of response for long time was checked, confirming consistent stability over long time range (180s). Transient photoresponse of PEC cell is the photovoltage rise and decay curve as shown in Fig.7b reveals that increase in photovoltage is almost instantaneous.

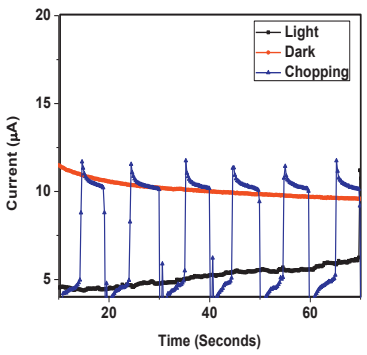

Fig. 7a. Speed of Response

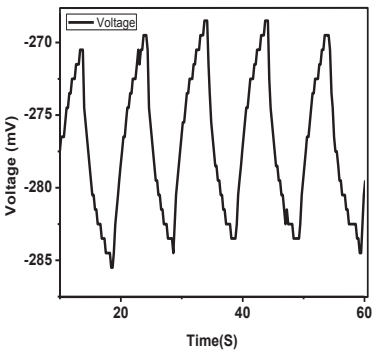

Fig. 7b. Photoinduced voltage as a function of time.

3.7. Capacitance–voltage (C–V) Characteristics and Electrochemical Impedance Spectroscopic (EIS) Study of PEC Cell

Capacitance measurement as a function of applied voltage (C–V) (Fig.8) gives useful information about photoelectrode such as type of conductivity, depletion layer width and flat band potential (V_{fb}). V_{fb} is an important factor in explaining charge transfer processes across the semiconductor–electrolyte junction and estimated from Mott–Schottky relation.

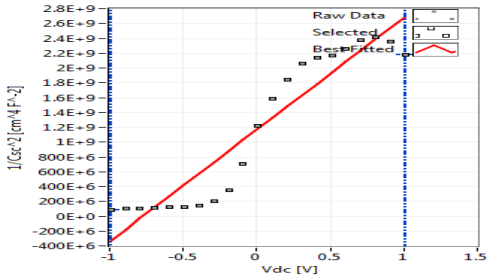

Fig.8 Mott–Schottky plot of PEC cell.

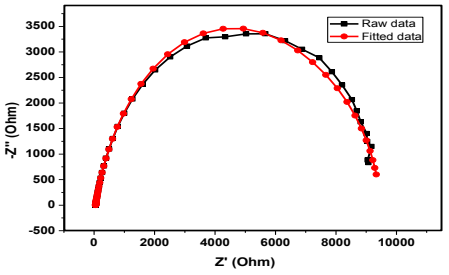

Fig.9 Nyquist plot for $ZnIn_2Se_4$ electrode

The variation of $1/C^2$ versus electrode potential (V) is non-linear as seen in Fig. 8, which is an indication of graded junction formation between $ZnIn_2Se_4$ and polysulphide electrolyte. Non-planar interfaces, surface roughness, presence of stacking faults due to irregular and sharp surface morphology, ionic adsorption on the film electrode surface may be the possible reasons for the deviation from linearity in C–V plot [25]. The value of the flat band potential obtained by extrapolating the straight line portion to the zero value was found to be −0. 8V/SCE for $ZnIn_2Se_4$–polysulphide redox electrolyte.

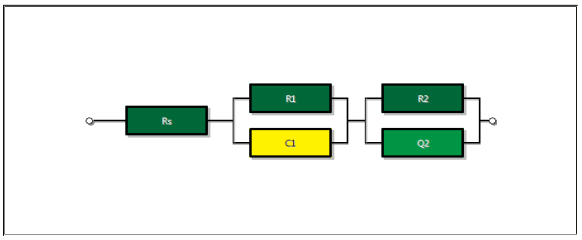

Fig. 10 The equivalent circuit derived from the Nyquist plot

The resultant EIS analysis generates a two-dimensional plot consisting of the real component (resistance) plotted along the abscissa and the imaginary component (impedance) along the ordinate. The nomenclature varies in the literature, however, these plots are commonly known as Nyquist or Cole-Cole plots [26].

The Nyquist plot of the $ZnIn_2Se_4$ at frequency 1 kHz is shown in Fig. 9. At high frequencies, the plot consists of a small semicircle, which is because of the charge-transfer resistance acting in parallel with the double layer capacitance.

Table 1. Component values of equivalent circuit.

Parameter	Value	Error
Rs	49 Ω	6.4
R1	1019.19Ω	10743.32
C1	0.002484 F	0.047381
R2	8431.614Ω	11644.95
Qy2	6.74E-05F	2.54E-05
Qa2	0.838F	0.0764

The Nyquist plot of the $ZnIn_2Se_4$ at frequency 1 kHz is shown in Fig. 9. At high frequencies, the plot consists of a small semicircle, which is because of the charge-transfer resistance acting in parallel with the double layer capacitance.

The equivalent circuit corresponding to $ZnIn_2Se_4$ electrode consists of C_1, R_1, Rs, R_2 and Q_2 elements, as shown in Fig.10. The C_1 is the pseudo capacitance, R_1 is the bulk resistance of the electrode, and R_2 is the charge transfer resistance. Table1. shows values of the components of equivalent circuit of the Nyquist plot.

4. Conclusions

In conclusion, a simple electrodeposition method has been used for the crystalline growth of n-type $ZnIn_2Se_4$ semiconductor film electrode consisting irregular and compact grains on stainless steel substrates from an aqueous acidic bath (pH~2) at ambient temperature. The X-ray diffraction measurement confirmed the crystalline quality of as-grown film electrode with tetragonal structure and preferential orientation along (2 2 0) plane. The PEC properties were studied in polysulphide electrolyte. $ZnIn_2Se_4$ film electrode show photovoltaic activity in polysulphide electrolyte, which promises a low cost device fabrication.

Acknowledgements

One of the authors B.G.Wagh gratefully acknowledges the contribution of the Pune University Research Fund under BCUD scheme.

References

[1] Sawant, R.R., Shinde, S.S., Bhosale, C.H. and Rajpure, K.Y., *Solar Energy,* 2010, 84, p. 1208-1214.
[2] Murali, K.R., Thilagavathy, K., Vasantha, S., Gopalakrishnan, P. and Oommen, P.R., *Solar Energy,* 2010, 84, p.722-728.
[3] Gracia, F.J., Tomar, M.S., *Thin Solid Films,* 1980, 69, p.137-142.
[4] Fillpowicz, J., Romeo, N. and L. Tarricone, *Solid State Commun*., 1980, 38, p.619-625.
[5] Yadav, S.P. , Shinde, P.S., Rajpure, K.Y. and Bhosale C.H., *Solar Energy,* 2010, 84, p. 1208-1215.
[6] Soliman, H.S. and El-Nahass, M.M. *Journal of materials science,*1991, 26, p. 1556-1558.
[7] Hendia, T.A. and Soliman, L.I. *Thin Solid Films,* 1995, 261, p.322-324.
[8] Nowak, E.,Neumann,H.,Scdumann,V and Steiner, B., *Physics stat. sol*. (a), 1992, 133, p.K13
[9] Xianzhong Sun, Yue He, Jiyayou Feng , *Journal of crystal growth,* 312, 2009,p. 48-56.
[10] Delahoy, A., Bruns, J., Liangfan, C., Akhtar, M., Kiss, Z. and Contreras, M., *Photovoltaic Specialists Conference, in: Conference Record of the 28th IEEE*, 2000, p.1437-1442.
[11] Ohtake, Y.,Okamoto, T., Yamada, A., Konagai, M and Saito, K., *Sol. Energy Mater. Sol. Cells,* 1997*,* 49, p.269-274.
[12] Ohtake, Y. , Chaisitsak, S., Yamada, A. and Konagai, M, *Jpn. J. Appl. Phys*.,1998, 37, p. 3220-3225.
[13] Sugiyama,M., Kinoshita, A., Miyama,A., Nakanishi,H. and Chichibu,S.F., *J. Cryst. Growth,* 2008, 310, p.794 -799.
[14] Yadav, S.P. , Shinde, P.S., Rajpure, K.Y. and Bhosale C.H., *Sol. Energy Mater. Sol. Cells,* 2008, 92, p. 453- 459.
[15] Yadav, S.P. , Shinde, P.S., Rajpure, K.Y. and Bhosale C.H., *J. Phys. Chem. Solids* , 2008, 69, p.1747- 1754.
[16] Choe, S.H., *Curr. Appl. Phys*., 2009, 9, p.1-4.
[17] Pourbaix, M., *Aqueous Stability Diagrams*, Atlas of Electrochemical Equilibria in Aqueous Solutions, Pergamon, London, 1966, p.39
[18] Brenner A., *Electrodeposition of Alloys Vol. 1*, Academic Press, New York, 1963, p. 12.
[19] Sartale, S.D. , Ganesan, V. and Lokhande,C.D., phys. stat. sol. (a), 2005, 202,No.1, p.85-96.
[20] McCandless BE and Hegedus SS, *Proc. of the 22th IEEE Photovoltaic Specialists Conference*, 1991, p.967-973.
[21] Zeyada, H.M., Aziz, M.S. and Behairy, A.S., Eur. *Phys. J. Appl. Phys.,* 2009, 45, p.30601-30604.
[22] Kale, S.S., Mane, R.S., Lokhande, C.D., Nandi, K.C. and Sung-Hwan Han, Mater. Sci. Eng., B,2006,133, p.222-226.
[23] Lokhande, C.D. and Pawar, S.H., *Mater. Chem. Phys*., 1984, 11, p. 201-209.
[24] Law, M. , Greene, L.E, Jhonson, J.C., Saykally, R. and Yang, P., *Nat.Mater*.,(2005,4, p. 455-461.
[25] Todkar,V.V., Mane, R.S., Lokhande, C.D. and Sung-Hwan Han, *J. Photochem. Photobiol, A*,2006, 181, p. 33-39.
[26] Justin, P., Meher, S.K. and Rao, G.R., *J. Phys. Chem. C,* 2010,114, pp.5203-5209.